Sorption Studies of Cs^+ and Ba^{2+} Cations on Magnesite

T. SHAHWAN, S. SUZER and H. N. ERTEN*

Department of Chemistry, Bilkent University, 06533 Bilkent, Ankara, Turkey

The adsorption behavior of Cs^+ and Ba^{2+} cations on magnesite has been studied as a function of time, cation concentration and temperature, utilizing both the radiotracer method and X-ray photoelectron spectroscopy (XPS). Saturation was approached in about 1 day for both cations. The sorption data were found to follow Freundlich type isotherms. Sorption of both Cs^+ and Ba^{2+} cations were found to be exothermic in nature with ΔH^0 (kJ/mol) of −37, −13 and ΔS^0 (kJ/mol·K) of −0.09, −0.009, respectively. Negative ΔG^0 values were obtained for both cations, indicating the spontaneity of their sorption on magnesite. The magnitude of ΔG^0 suggest that ion exchange is the dominating sorption mechanism. © 1998 Elsevier Science Ltd. All rights reserved

Introduction

In order to provide the necessary protection for the environment, nuclear wastes could be disposed of, in deep or shallow geological repositories. Clay minerals have been proposed as suitable backfilling materials in these repositories, because of their ability in retarding or delaying the migration of radionuclides to the biosphere (Jedinakova-Krizova, 1996). Thus, sorption studies investigating how the interactions between the clays and the radionuclides are affected by various factors that control the sorption process become quite important. Among such factors are the concentration of radionuclides in groundwater, the period of contact, the temperature, pH, the size of clay particles and the liquid–solid ratio.

Many investigations have been carried out to examine the effect of such factors on the sorption and transport properties of different radionuclides (Rafferty *et al.*, 1981; Torstenfelt, 1986; Benes *et al.*, 1989; Lieser, 1995). Detailed work examining the sorption/desorption behavior of Cs^+ and Ba^{2+} ions on different clays and soil fractions from various regions of Turkey was carried out (Erten *et al.*, 1988; Eylem *et al.*, 1990) In those studies, sorption of Cs^+ and Ba^{2+} cations on magnesite was examined as a function of time, cation concentration and temperature. The interaction of Cs^+ with various soil fractions is of considerable interest in radioactive waste considerations. The radionuclide ^{137}Cs is produced in high yield during the fission process

and due to its long half life ($t_{1/2} = 30.17$ years), is a principal radiocontaminant. ^{140}Ba ($t_{1/2} = 12.8$ days) is also a serious radiocontaminant during the first 100 days when fission products are discharged into the environment. Furthermore Ba being a homologue of Ra is a suitable cation for the radiochemical study of Ra, a serious contaminant in some radioactive wastes. ^{133}Ba was chosen as a tracer because of its long half life (10.7 years) and easily measurable γ-ray (361 keV). Magnesite, a mineral composed mainly of magnesium carbonate with minor amounts of quartz with a single exchangeable cation (Mg^{2+}), was chosen as the solid phase for this study. Mineral samples were separated into various size fractions by dry and wet sieving. The particle size of the samples used was less than 75 μm. The cation exchange capacity (CEC) of magnesite determined by the silver–thiourea method was 3–7 - meq/100 g (Searle, 1986).

X-ray photoelectron spectroscopy (XPS), an inherently surface sensitive technique, is among the few methods available for direct chemical and structural characterization of mineral surfaces. The XPS spectrum provides information about the elemental composition and chemical speciation of the sample analyzed. XPS is a clear and well-defined analytical technique based on the positions and intensities of peaks within the spectrum. Furthermore, the exact positions of the peaks are related to the chemical environment of the electrons, so that additional structural and chemical information can be deduced from binding energy shifts. Many studies of the interactions between radionuclides and different mineral matrices have used this powerful tool

---

*To whom all correspondence should be addressed.

Table 1. Concentrations of primary cations in laboratory tapwater used in sorption studies

Cation	Na$^+$	K$^+$	Ca^{2+}	Mg^{2+}
Concentration (meq/ml)	3.54×10^{-4}	1.21×10^{-4}	2.67×10^{-4}	4.38×10^{-4}

Table 2. Initial cation concentrations of Cs$^+$ and Ba^{2+} used in studying the effect of loading and temperature on sorption

Cation	Concentration (meq/ml)					
Cs$^+$	1.00×10^{-1}	1.00×10^{-2}	1.00×10^{-3}	1.00×10^{-4}	1.00×10^{-5}	1.00×10^{-6}
Ba$^+$	—	1.07×10^{-2}	2.15×10^{-3}	—	1.00×10^{-5}	1.00×10^{-6}

(Koppelman *et al.*, 1980; Dillard and Koppelman, 1992). In this study the sorption affinities of magnesite towards cesium and barium ions are examined.

Experimental

Radiotracer method

For the radiotracer experiments, aliquots of 30 mg of magnesite (obtained from the Turkish Mining Institute MTA) were weighed out into a pre-weighed tube and 3 ml of laboratory tapwater as substitute for groundwater were added into each tube which was then shaken for 4 days with a lateral shaker at 125 rpm. Samples were then centrifuged at 6000 rpm for 30 min and the liquid phases were discarded. Each tube was then weighed to determine the amount of water remaining inside after discarding the decantate (ΔW_{pt}). This pretreatment step was intended to mimic the equilibrium situation of the magnesite samples with groundwater prior to sorption experiments. The powders were later used in the sorption experiments. The cation composition of Bilkent tapwater used in the sorption experiments is given in Table 1.

Kinetic studies. To each of the 30 mg pretreated magnesite samples, 3 ml of solutions containing 1×10^{-4} meq/ml of Cs$^+$ or Ba^{2+} with appropriate amounts of ^{137}Cs or ^{133}Ba radiotracers were added.

Sample tubes were shaken at room temperature for periods ranging from 1 h to 7 days. Samples were then centrifuged and 2 ml portions of the liquid phases were counted using a 35 cm^3 calibrated Ge detector connected to a multichannel analyzer. Two samples were measured for a point.

Effect of loading and temperature. The effect of temperature on sorption was studied for each of the initial cation concentrations given in Table 2. Experiments were carried out at four different tem-
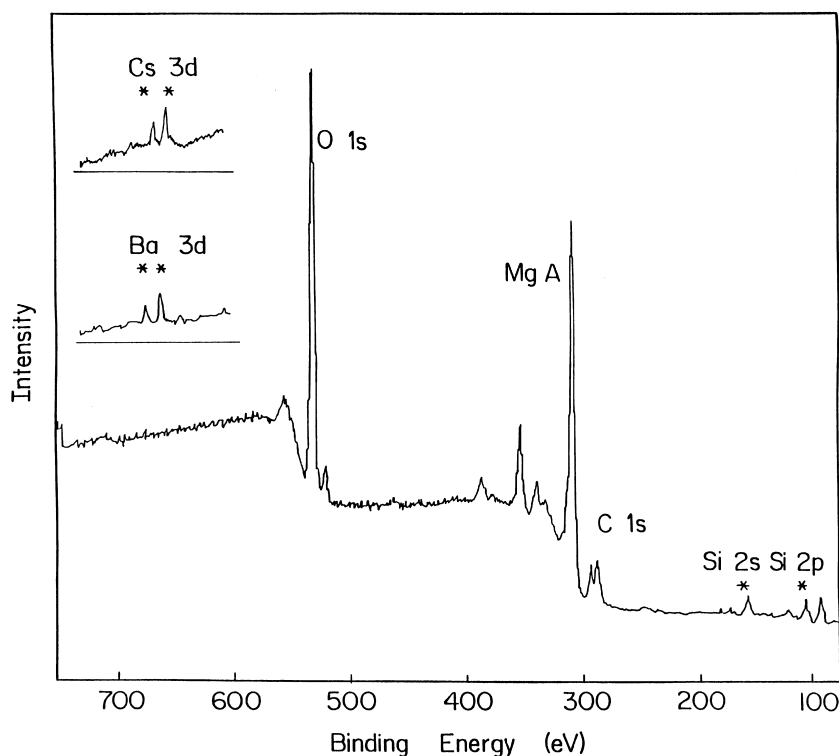

Fig. 1. Photoelectron spectra of magnesite before sorption and Cs and Ba 3d regions after sorption of Cs$^+$ and Ba^{2+} ions on magnesite.

peratures: 30, 40, 50 and 60°C. 3 ml of the cation solution of interest containing an appropriate amount of radiotracer was added to each sample tube containing 30 mg of magnesite at the desired temperature. The samples were shaken for 1 day, centrifuged and 2 ml portions of the liquid phase were counted.

Analysis by XPS

The XPS technique was used in this study to carry out qualitative and quantitative analysis of the nature and extent of sorption in the samples. The elemental contents of the samples were identified from the peaks in the XPS spectrum. The intensities of these peaks were proportional to the elemental concentrations of the atoms or ions within the sample. The spectra were recorded using a KRATOS ES-300 spectrometer (AEI instruments, Manchester, England) with an Al K_α ($h\upsilon = 1486.3$ eV) source. Samples were introduced as powders pressed on to adhesive copper tapes and the pressure in the analyzer chamber was kept below 10^{-8} Torr during analysis. For calibration purposes the C 1s line (B.E = 285.0 eV) was used. This peak arises in the spectra as a result of residual or deposited hydrocarbons on the surface. The silicon content was assumed to be constant before and after the exchange, therefore the Si 2p peak was used to normalize the intensity of the peaks belonging to other elements. The normalized intensities were then used to calculate the atomic ratios utilizing the formula (Chastain, 1992):

$$[A]/[B] = (I_A/I_B)(\sigma_B/\sigma_A)(E_k(B)/E_k(A))^{3/2} \quad (1)$$

where $[A]/[B]$ is the atomic ratio of A and B, I is the observed intensity, σ is the tabulated cross section (Scofield, 1976) and E_k is the kinetic energy ($h\upsilon -$ B.E) of the electrons emerging from the analyzed sample.
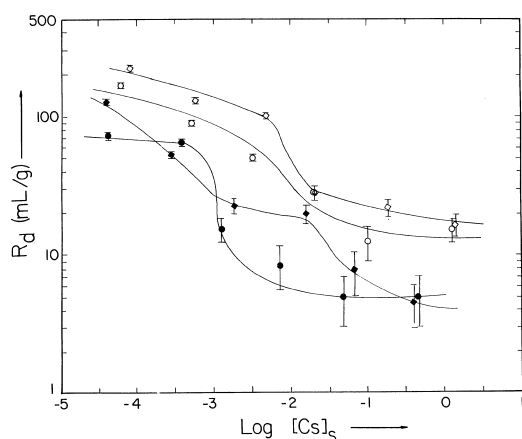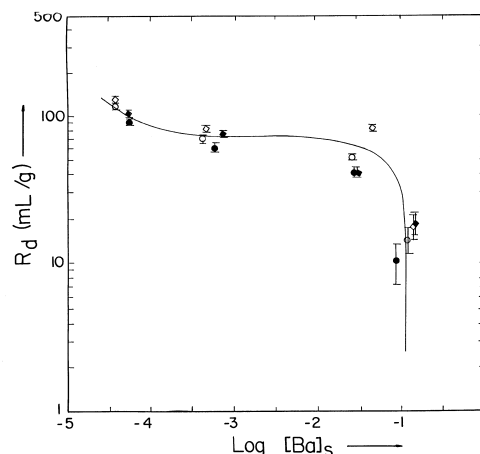

Fig. 3. Variation of R_d as a function of barium ion loading (meq/g) at various temperatures obtained by the radiotracer method. $\Diamond$: $T = 30°C$, $\bigcirc$: $T = 40°C$, $\blacklozenge$: $T = 50°C$, $\bullet$: $T = 60°C$.

Kinetic studies. 3 ml portions of the 0.1 M Cs^+ or Ba^{2+} solutions were added to 30 mg magnesite samples, without radiotracer. Sorption was carried out at room temperature for periods starting from 1 h up to several days. Mineral samples were then filtered and dried at 60°C for 24 h. Then the XPS spectra were recorded, the Cs and Ba $3d_{5/2}$ peak areas were used to calculate the atomic concentrations of each species in the samples.

Effect of concentration. To 30 mg magnesite samples 3 ml portions of solutions containing 1, 0.1, 0.01, 0.001 M of Cs^+ or Ba^{2+} cations were added in each case. Sorption was carried at room temperature for 1 day by shaking. Samples were then filtered, dried and their XPS spectra were recorded.

Effect of temperature. To study the temperature effect on sorption, experiments were performed at 30, 40, 50, 60 and 70°C. 3 ml 0.1 M cation solutions were added to 30 mg magnesite samples both of which were previously brought to the desired temperature and the samples were shaken for 1 day.
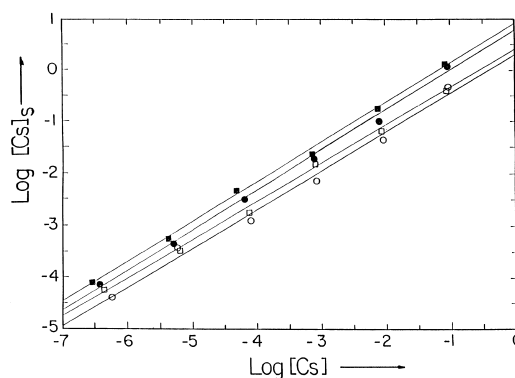

Fig. 2. Variation of R_d as a function of cesium ion loading (meq/g) at various temperatures obtained by the radiotracer method. $\Diamond$: $T = 30°C$, $\bigcirc$: $T = 40°C$, $\blacklozenge$: $T = 50°C$, $\bullet$: $T = 60°C$.

Fig. 4. Freundlich isotherm plots of cesium ion sorption on magnesite at different temperatures. $\blacksquare$: $T = 30°C$, $\bullet$: $T = 40°C$, $\square$: $T = 50°C$, $\bigcirc$: $T = 60°C$.
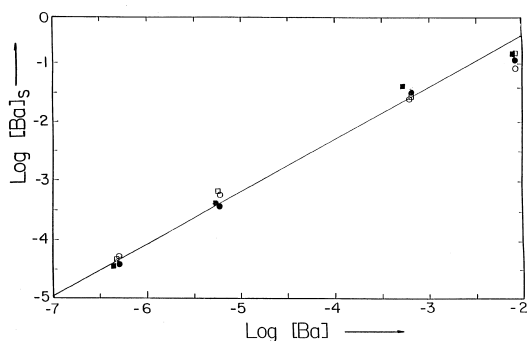
Fig. 5. Freundlich isotherm plots of barium ion sorption on magnesite at different temperatures. ■: $T = 30°C$, •: $T = 40°C$, □: $T = 50°C$, ○: $T = 60°C$.

The phases were then separated by filtration, dried and the XPS spectra were recorded.

The distribution ratio. The distribution ratio of adsorption is defined as:

$$R_{d,ad} = \frac{[C]_{s,ad}}{[C]_{ad}}. \tag{2}$$

Where $[C]_{s,ad}$ (meq/g) and $[C]_{ad}$ (meq/ml) are the concentrations of species C in the solid and liquid phases, respectively. At the beginning of the sorption step, V (ml) of solution with initial concentration $[C]^0$ (meq/ml) is used and at the end of the sorption step $V + \Delta W_{pt}$ (ml) of solution with concentration $[C]_{ad}$ are present, hence the concentration of C in the solid phase after sorption can be expressed as:

$$[C]_{s,ad} = \frac{V[C]^0 - (V + \Delta W_{pt})[C]_{ad}}{W_s}. \tag{3}$$

In terms of radioactivity, $[C]_{ad}$ can be written as:

$$[C]_{ad} = \frac{A_{l,ad}}{A^0}[C]^0. \tag{4}$$

From (1)–(3), the following equation is obtained:

$$R_{d,ad} = \frac{VA^0 - (V + \Delta W_{pt})A_{l,ad}}{A_{l,ad}W_s} \tag{5}$$

where A^0 = initial count rate of solution added for sorption (cps)/ml, $A_{l,ad}$ = count rate of solution after sorption (cps)/ml, W_s = weight of solid material (g) and ΔW_{pt} = amount of liquid remaining in the tube after pretreatment, before sorption (g).

Results and Discussion

The XPS spectrum of magnesite excited by Al K_α X-rays ($h\upsilon$ = 1486.3) before sorption and the relevant regions of the spectrum after Cs^+ and Ba^{2+} sorption are shown in Fig. 1. The spectrum provides qualitative and quantitative information about the species involved. Mg A refer to the KLL Auger lines of Mg and one C 1s peak arises from CO_3^{2-} (the other one is due to the presence of some hydrocarbons). These peaks originate from the major component of magnesite, $MgCO_3$, the Si 2s and 2p peaks belong to quartz the minor component of magnesite.

Kinetic studies

The results of the effect of time on sorption carried out using both the radiochemical and XPS methods have shown that for both cations saturation was approached in about one day of contact. The rapid uptake of both Cs^+ and Ba^{2+} ions indicate that fast adsorption steps are involved and that
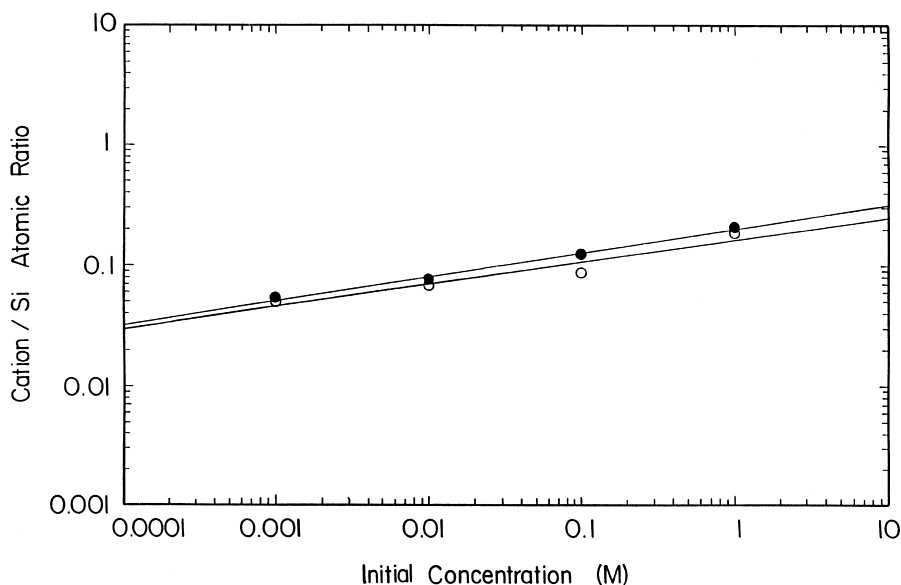

Fig. 6. Change of the atomic ratio of cation (cation/Si) with the initial cation concentration (M) obtained by X-ray photoelectron spectroscopy. ○: Barium ion, •: cesium ion.

Table 3. Parameters for the Freundlich type isotherm fits to the data for the sorption of Cs$^+$ and Ba^{2+} cations on magnesite at different temperatures

Temperature (K)	Cs$^+$		Ba^{2+}	
	k (meq/g)	n	k (meq/g)	n
303	7.9	0.77	16.2	0.87
313	4.0	0.75	10.4	0.85
323	2.4	0.74	9.1	0.81
333	1.8	0.74	5.9	0.80

ion exchange at the surface could be the dominating adsorption mechanism.

Effect of loading and temperature

The R_d values obtained by the radiotracer method for the sorption of Cs$^+$ and Ba^{2+} on magnesite with various initial concentrations at different temperatures are plotted as a function of cation loading in Figs 2 and 3. The error bars represent calculated uncertainties resulting from weight, volume and activity measurements using the standard propagation of errors relationships. As illustrated in Fig. 2, the curves show characteristic inverse S-shapes indicating that two different exchange sites on the solid matrix are present in the case of Cs$^+$ sorption. On the other hand, Fig. 3 suggests that a single exchange site is present in the case of Ba^{2+} sorption. The sorption of Cs$^+$ is seen to be temperature dependent whereas Ba^{2+} sorption is little affected by temperature changes. Since the R_d values obtained for the different Ba^{2+} ion concentrations do not show significant changes at different temperatures, a single curve was used to represent the data. The curves were drawn to guide the eye. Figures 4 and 5 illustrate Freundlich isotherm plots of the data obtained by the radiotracer method at various temperatures for the sorption of Cs$^+$ and Ba^{2+} ions, respectively. It is seen that Freundlich type isotherms provide an adequate description of the sorption behavior in all cases. The results obtained by XPS are shown in Fig. 6. It is seen that the amount of cations adsorbed increases with increasing initial concentration. The results are also in line with those shown in Figs 4 and 5.

The Freundlich type isotherm at a particular temperature may be described as:

$$[C]_{s,ad} = k[C]_{ad}^n. \qquad (6)$$

Where $[C]_{s,ad}$ is the amount of ionic species adsorbed on the solid matrix at equilibrium (meq/g), $[C]_{ad}$ is the concentration of the cation in solution at equilibrium (meq/ml), k and n are Freundlich constants. The results of least square fits to the experimental data are given in Table 3. A higher value of k indicates higher sorption affinity for the ion in solution, whereas a higher value of n indicates higher sorption intensity (Mishra and Tiwary, 1995). At the limit when $n = 1$, the adsorption is said to be linear and the constant k becomes equivalent to R_d.

It is interesting to observe that the Ba^{2+} ion has both higher affinity and higher intensity of adsorption than the Cs$^+$ ion. This is probably due to the fact that the exchanging cation Mg^{2+} has a divalent positive charge as Ba^{2+}. Furthermore, the n values seem to be independent of temperature, whereas the k values show a drastic decrease with increasing temperature for both species.

Effect of temperature

Arrhenius plots, that is the change of ln R_d values with reciprocal temperature, can be plotted using the equation (Qadeer *et al.*, 1993):

$$\ln R_d = \frac{\Delta S^0}{R} - \frac{\Delta H^0}{RT} \qquad (7)$$

where R is the gas constant, 8.314 J/mol·K, ΔH^0, ΔS^0 are the enthalpy and entropy changes associated with the sorption process and T is the sorption temperature (K). Figures 7 and 8 show Arrhenius plots for Cs$^+$ and Ba^{2+} sorption, respectively. The linear correlation coefficients for the different concentrations of Cs$^+$ ion range from 0.889 to 0.995 and those of Ba^{2+} ion range from 0.830 to 0.959. It was observed that the values of R_d decrease with increasing temperature. The decrease for the Cs$^+$ ion is more pronounced than that for the Ba^{2+} ion.

Thermodynamic parameters such as the enthalpy change, ΔH^0, and entropy change, ΔS^0, in sorption,

Fig. 7. Variation of log R_d as a function of temperature for the sorption of cesium ion on magnesite at various initial ion concentrations (meq/ml). ●: 1.00×10^{-1}, ■: 1.00×10^{-2}, ▲: 1.00×10^{-3}, ◆: 1.00×10^{-4}, ▼: 1.00×10^{-5}, ○: 1.00×10^{-6}.
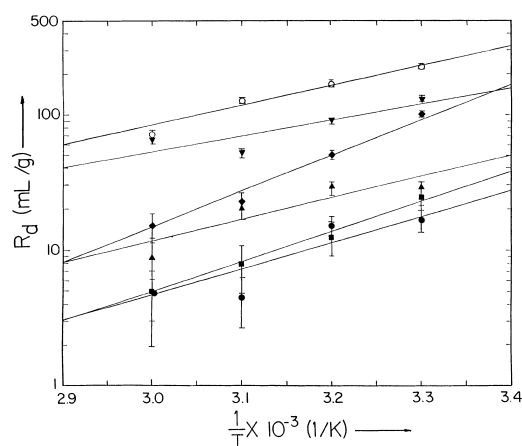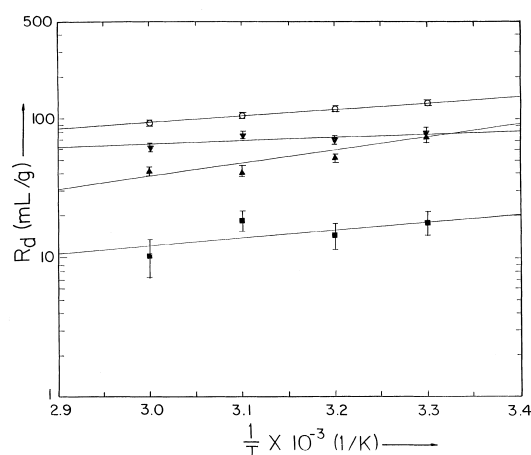
Fig. 8. Variation of log R_d as a function of temperature for the sorption of barium ion on magnesite at various initial ion concentrations (meq/ml). ■: 1.07×10^{-2}, ▲: 2.15×10^{-3}, ▼: 1.00×10^{-5}, ○: 1.00×10^{-6}.

were calculated from the slopes and intercepts of least square fits to the experimental data. The linear correlation coefficients for the different concentrations of Cs^+ ion range from 0.889 to 0.995 and those of Ba^{2+} ion range from 0.830 to 0.959.

The thermodynamic parameters ΔH^0 and ΔS^0 for the sorption of Cs^+ and Ba^{2+} ions on magnesite obtained in this work are given in Table 4. These values were averaged for the different concentrations and the uncertainties represent standard deviations (S.D.).

The negative values for the enthalpy change, ΔH^0, indicate the exothermic nature of sorption. A decrease in temperature favors the sorption of products which are energetically stable. The decrease in adsorption with the rise in temperature may be due to increased desorption as a result of the increase in the thermal energy of the adsorbates (Panday et al., 1984). The negative value of the entropy change, ΔS^0, is an indication of the stability of surface adsorption. The relatively lower negative value of ΔS^0 is indicative of the presence of high energy bonds and an ordered arrangement of the adsorbate over the adsorbent (Sundaram, 1994). Thus, Cs^+ ions exhibit stronger binding to magnesite and their arrangement is more ordered than Ba^{2+} ions.

The free energy of specific adsorption, ΔG^0 was calculated for different concentrations at each temperature utilizing the following equation:

$$\Delta G^0 = -RT \ln R_d. \qquad (8)$$

The calculated values of ΔG^0 were similar for both cations at all four temperatures, averaging 9 ± 3 (S.D.) (kJ/mol) for Cs and 10 ± 2 (S.D.) (kJ/mol) for Ba. The spontaneity of the exchange process is indicated by the negative ΔG^0 values for both of the cations. The magnitude of the energy of sorption is in the 8–16 kJ/mol range which is the energy range for ion exchange type reactions (Helferich, 1964). Thus, the mechanism of both Cs and Ba ion sorption on magnesite is principally an ion exchange.

Surveying the literature, it was found that few studies on the sorption of Cs^+ and Ba^{2+} ions on various minerals at different temperatures were carried out. Sorption of Cs^+ ion on alumina was seen to be exothermic, with the thermodynamic parameters being of the same order of magnitude as we have obtained in this study (Khan et al., 1995).

Conclusions

The following conclusions about the sorption of cesium and barium ions on magnesite can be drawn:

— Radiotracer and XPS studies indicate that for cesium and barium sorption on magnesite, equilibrium is established within a day of contact.

— For cesium, sorption takes place primarily via two mechanisms and/or exchanging sites. This is indicated by the inverse S-shape loading curves. On the other hand, sorption of barium occurs via a single mechanism as suggested by the single plateau loading curve.

— The XPS studies show that the atomic concentration ratio and hence the surface coverage increases as the cation initial concentration increases for both cesium and barium ion sorption.

— Freundlich isotherms, as compared to other isotherm types provide the most adequate description of the sorption data for Cs^+ and Ba^{2+} ions at different temperatures. The values of Freundlich parameters k and n suggest that Ba^{2+} ion has a larger sorption affinity and intensity.

— The negative values and magnitudes of ΔH^0 and ΔS^0 for both ions indicate the exothermic and stable nature of adsorption. The lower ΔS^0 value for Cs^+ suggests a more ordered and stable adsorption. Negative ΔG^0 values show that the adsorption process is spontaneous. The magnitudes of ΔG^0 for both cations at all the temperatures studied suggest that ion-exchange is the main adsorption mechanism.

Table 4. The average values of the thermodynamic parameters ΔH^0 and ΔS^0 in the adsorption of Cs^+ and Ba^{2+} ions on magnesite obtained in this work

Cation	ΔH^0 (kJ/mol)	ΔS^0 (kJ/mol·K)
Cs^+	-37 ± 5	-0.09 ± 0.04
Ba^{2+}	-13 ± 5	-0.009 ± 0.002

References

Benes, P., Lam Ramos, P. and Poliak, R. (1989) Factors affecting interactions of radiocesium with freshwater solids, pH, composition of water and solids. J. Radioanal. Nucl. Chem. **133**, 359.

Chastain, J. (1992) Handbook of X-ray Photoelectron Spectroscopy. Perkin-Elmer Co.

Dillard, J. G. and Koppelman, M. H. (1992) X-ray photo-electron spectroscopy (XPS) surface characterization of cobalt on the surface of kaolinite. *J. of Colloid and Interface Science* **87,** 46.

Erten, H. N., Aksoyoglu, S. and Gokturk, H. (1988) Sorption/desorption of Cs on clay and soil fractions from various regions of Turkey. *Sci. Total Environ.* **69,** 269.

Eylem, C., Erten, H. N. and Gokturk, H. (1990) Sorption–desorption behavior of barium on clays. *J. Environ. Radioactivity* **11,** 183.

Helferich, F. (1964) *Ion-Exchange.* McGraw-Hill, New York.

Jedinakova-Krizova, V. (1996) Radionuclides migration in the geosphere and their sorption on natural sorbents. *J. Radioanal. Nuc. Chem.* **208,** 559.

Khan, S. A., Reman, R. Ur. and Khan, M. A. (1995) Adsorption of Cs(I), Sr(II) and Co(II) on Al_2O_3. *J. Radioanal. Nuc. Chem.* **190,** 81.

Koppelman, M. H., Emerson, A. B. and Dillard, J. G. (1980) Adsorbed Cr(III) on chlorite, illite and kaolinite: An X-ray photoelectron spectroscopic study. *Clays and Clay Minerals* **28,** 119.

Lieser, K. H. (1995) Radionuclides in the geosphere: Sources, mobility, reactions in natural waters and interactions with solids. *Radiochim. Acta* **70–71,** 355.

Mishra, S. P. and Tiwary, D. (1995) Ion exchangers in radioactive waste management. *Radioanal. Nucl. Chem.* **196,** 353.

Panday, K. K., Prasad, G. and Singh, V. N. (1984) Removal of Cr(VI) from aqueous solutions by adsorption on fly ash-wollastonite. *J. Chem. Technol. Biotechnol.* **34A,** 367.

Qadeer, R., Hanif, J., Saleem, M. and Afzal, M. (1993) Surface characterization and thermodynamics of adsorption of Sr^{2+}, Ce^{3+}, Sm^{3+}, Gd^{3+}, Th^{4+}, UO_2^{2+} on activated charcoal from aqueous solutions. *Colloid Polym. Sci.* **271,** 83.

Rafferty, P., Shiao, S. Y., Binz, C. and Meyer, R. (1981) Adsorption of Sr(II) on clay minerals: Effect of salt concentration, loading and pH. *J. Inorg. Nucl. Chem.* **43,** 797.

Scofield, J. H. (1976) Hartree–Slater subshell photoionization cross sections at 1254 and 1487 eV. *J. Electr. Spect.* **8,** 129.

Searle, P. L. (1986) The measurement of soil cation exchange properties using the single extraction, silver thiourea method. *Aust. J. Soil Res.* **24,** 193.

Sundaram, K. M. S. (1994) Adsorption behavior of RH-5992 insecticide onto sandy and clay loam forest soils. *J. Environ. Sci. Health. B* **29** (3), 415.

Torstenfelt, B. (1986) Migration of fission products strontium, technitium, iodine and cesium in clay. *Radiochim. Acta* **39,** 97.